HEP'99 # 5_515
Submitted to Pa 5
Pl 5

DELPHI 99-104 CONF 291
15 June 1999

A measurement of the branching fractions of the b-quark into strange, neutral and charged B-mesons

Preliminary

DELPHI Collaboration

Paper submitted to the HEP'99 Conference
Tampere, Finland, July 15-21

A measurement of the branching fractions of the b-quark into strange, neutral and charged B-mesons

Preliminary

M Feindt [1], **C. Weiser** [2]

Abstract

The production rates of B_s^0, B_d^0 and B^+ mesons in b-quark events have been measured with the DELPHI detector at LEP. For the B_s^0 rate, the properties of the fragmentation kaon accompanying the heavy meson have been used. The description of the fragmentation process in the simulation has been verified with exclusively reconstructed D-mesons in c-quark events. To determine the rate of charged and neutral B-mesons, an algorithm has been developed, based on a neural network, to estimate the charge of the weakly decaying B-meson through distinguishing decay particles from their fragmentation counterparts.

[1] University of Karlsruhe

[2] CERN

1 Introduction

The branching ratios of the b-quark into the different species of b-hadrons are an important input for many measurements, e.g. B-oscillation analyses. A direct measurement of these quantities using exclusive decays is difficult, since there are many decay channels with small branching fractions having large relative uncertainties [1]. The averages for weakly decaying b-hadrons are performed by the LEP B oscillation working group [2]. The input used for the estimation of f_{B_S}, the fraction of weakly decaying B_s^0-mesons, are measurements of the product branching ratio $Br(\bar{b} \to B_s^0) \cdot Br(B_s^0 \to D_s^- l^+ \nu X)$ [3] and information from mixing measurements. This results in $f_{B_S} = (10.8 \pm 1.4)\%$. The baryon rate is estimated from similar products, using $\Lambda_c^+ l^-$ and $\Xi^- l^-$ correlations [4], and a measurement of proton production in b-hadron decays [5], leading to $f_{b-baryon} = (10.2^{+2.3}_{-2.1})\%$. For non strange B-mesons one gets, assuming isospin symmetry and thus equal production rates for B_d^0, B^+ [1] and $\sum f_{B-species} = 1$, $f_{B_d^0} = f_{B^+} = (39.5^{+1.3}_{-1.4})\%$. No direct measurements of f_{B_d} or $f_{B_u^+}$ have been published so far. In this paper, an analysis of the data taken with the DELPHI detector at LEP in the years 1994 and 1995 is presented [2], which measures the fractions f_{B_s} and $f_{B_d^0,B^+}$ in an inclusive way. The properties of the fragmentation kaon accompanying the strange heavy meson have been exploited to measure the fraction of primary produced strange b-hadrons. To reduce the dependence of fragmentation models, properties of fragmentation tracks have been studied using exclusively reconstructed D-mesons in a sample of $c\bar{c}$ enriched events. For the rates of neutral and charged b-hadrons, an efficient algorithm has been developed to distinguish tracks from B-decays from their fragmentation counterparts. This allows an estimate of the charge of the weakly decaying hadron.
In figure 1 a schematic picture of the b-hadron production process is shown. In table 1 the b-hadron rates of the JETSET Monte-Carlo model are summarised. The simulation used the JETSET 7.3 model [6] with parton shower option and parameters determined from earlier QCD studies [7], followed by a detailed detector simulation [8].
All results presented in this paper are preliminary.

2 The Experimental Procedure and Event Selection

The DELPHI detector is described in detail in references [9, 10]. The present analysis relies on information provided by the central tracking detectors and the Ring Imaging Cherenkov detectors.

- The **microVertex Detector** (VD) consists of three layers of silicon strip detectors at radii of 6.3, 9.0 and 10.9 cm. $R\Phi$ coordinates in the plane perpendicular to the beam are measured in all three layers. The first and third layers also provide Z information (from 1994 on). The polar angle (θ) coverage for a particle passing all three layers is from 44° to 136°. The single point resolution has been estimated from

[1] The presence of B*-mesons does not, contrary to the D-system, change the rates of charged and neutral B-mesons, because their dominant decay mode is $B^* \to B\gamma$. This is also the case for orbitally excited B**-mesons, if $f_{B^{**0}} = f_{B^{**+}}$, and isospin rules are used to calculate the dominant single pion transitions.

[2] For the analysis described in chapter 5 only the data of the year 1994 have been used.

Type	Q	f': Fragmentation [%]	f: Weak decay [%]
non-strange mesons	0,±1	79.8 ($B^{(*)}$,B^{**})	83.7 (B)
	±1	39.9 ($B_u^{(*)}$,B_u^{**})	41.8 (B_u)
	0	39.9 ($B_d^{(*)}$,B_d^{**})	41.8 (B_d)
	0,±1	28.0 (B^{**})	
strange mesons	0	11.1 ($B_s^{(*)}$,B_s^{**})	7.3 (B_s)
	0	3.9 (B_s^{**})	
non-strange baryons	0,±1	7.9	7.9
	0	4.9 ($\Lambda_b, \Sigma_b^{(*)}$)	7.9 (Λ_b)
	±1	3.0 ($\Sigma_b^{(*)}$)	
strange baryons	0,±1	1.2	1.2
	0	0.6 ($\Xi_b^{(*)}$)	0.6 ($\Xi_b^{(*)}$)
	±1	0.6 ($\Xi_b^{(*)}, \Omega_b$)	0.6 ($\Xi_b^{(*)}, \Omega_b$)

Table 1: The b-hadron production rates of the JETSET 7.3 Monte-Carlo model with parton shower option and parameter settings according to DELPHI-Tuning [7]. The rates f' of hadrons produced in the fragmentation process and the rates f of weakly decaying b-hadrons are shown. The parameters giving the suppression of $s\bar{s}$ pairs and diquarks are, respectively, $\gamma_s = P(s\bar{s})/P(u\bar{u}) = P(s\bar{s})/P(d\bar{d})$=0.28 and $P(qq)/P(q)$=0.1.

real data to be about 8 μm in $R\Phi$ and (for charged particles crossing perpendicular to the module) about 9 μm in Z.

- The **Inner Detector** (ID) consists of an inner drift chamber with jet chamber geometry and 5 cylindrical MWPC layers. The jet chamber, between 12 and 23 cm in R and 23° and 157° in θ, consists of 24 azimuthal sectors, each providing up to 24 $R\Phi$ points. Since 1995, a longer ID has been operational. The polar angle coverage now is from 15° to 165°.

- The **Time Projection Chamber** (TPC) is the main tracking device of DELPHI. It provides up to 16 space points per particle trajectory for radii between 40 and 110 cm and polar angles between 39° and 141°. The precision on the track elements is about 150 μm in $R\Phi$ and about 600 μm in Z. For particle identification a measurement of the specific energy loss dE/dx is provided by 192 sense wires located at the end caps of the drift volume.

- The **Outer Detector** (OD) consists of 5 layers of drift tubes between radii of 197 and 206 cm. Its polar angle coverage is from 42° to 138°. The OD provides 3 space points and 2 $R\Phi$ points per track.

- The **Ring Imaging CHerenkov counters** (RICH) provide additional information for particle identification measuring the Cherenkov light, emitted by particles traversing a dielectric medium faster than the speed of light. The barrel part of the detector covers the polar angle from 40° to 140°. To cover a large momentum range, one liquid (C_6F_{14}) and one gas (C_5F_{12}) radiators are used.

An event has been selected as multihadronic if the following requirements are satisfied:

- There must be at least 5 charged particles in the event, each with momentum larger than 400 MeV/c and polar angle between 20° and 160°.
- The total reconstructed energy of these charged tracks has to exceed 12% of the centre of mass energy (assuming all particles to have the pion mass).
- The total energy of the charged particles in each hemisphere (defined by the plane perpendicular to the beam axis) has to exceed 6% of the beam energy.

After these cuts, about 2 Million events from the 1994 and 1995 runs have been selected. About 4 Million simulated $Z^0 \to q\bar{q}$ events have been selected with the same cuts.

2.1 Tagging $b\bar{b}$ events

The most important variables to tag or antitag $b\bar{b}$ events are the impact parameters of charged tracks with respect to the primary vertex which is fitted on an event by event basis using position and size of the beamspot as constraints. The output is a probability, that a selected sample of tracks originate from the primary vertex. Thus, to select $b\bar{b}$ events, one requires low values of this probability. This method is described in detail in [10]. To increase the efficiency, additional variables like the track momenta and angles with respect to their jet axis can be used. A description of this so called 'B confidence method' can be found in [11]. Here, the hypothesis is tested, that an event or a hemisphere originates from a given type of quark. Thus, one requires values close to 1 for the b-quark hypothesis to enrich the selected sample in $b\bar{b}$ events.

2.2 Hadron identification

For the identification of charged hadrons combined information provided by the TPC and the barrel RICH is used. The tagging routine is based on probabilities for each particle hypothesis evaluated separately for the gas and liquid radiator of the RICH and the dE/dx measured in the TPC. For different efficiencies and purities three tags exist for the hypotheses, namely 'loose', 'standard' and 'tight', where 'tight' gives the lowest efficiency and the best background reduction.

3 Measurement of the strange b-hadron rate

The absolute values of exclusive branching ratios of B_s^0 mesons are unknown and more inclusive ones, like $B_s^0 \to D_s^- l^+ \nu_l X$ have large uncertainties. A measurement of these quantities is difficult, because the number of produced B_s^0-mesons has to be known with a certain accuracy. As a consequence, using exclusive or inclusive B_s^0-decays to give an estimate for the B_s^0-rate in $b\bar{b}$ events at $\sqrt{s} = m_Z$ is not possible with small errors. The presence of $B^0 - \bar{B}^0$ oscillations made it possible to measure f_{B_s} with some accuracy, because the oscillation rate is different for B_d^0 and B_s^0-mesons. Thus, comparing measurements at the $\Upsilon(4S)$ resonance, where no B_s^0-mesons are produced, with LEP measurements gives sensitivity to f_{B_s}. Since the origin of B^0-oscillations is the weak interaction,

this measurement is sensitive to the rate of weakly decaying B_s^0-mesons. In the present analysis a different approach is used which is based on fragmentation properties of b-jets and which is sensitive to the total rate of strange b-hadrons produced in jets.
In the string fragmentation model, invented by the LUND group, which has been shown to be very successful to describe experimental data, a B_s^0-meson is created in the following way: the $\bar{b}$-quark produced in the decay of the Z^0 picks up a s-quark which has been created together with a $\bar{s}$-quark during the breakup of the string, originally being stretched between the $b\bar{b}$ pair. Due to the local strangeness compensation in this picture, the following particle which is produced in the fragmentation chain, will contain the $\bar{s}$-quark, as shown in figure 2a. Depending on the flavour of the quark pair which is created in the following breakup of the string, a neutral or positively charged hadron is formed. This hadron may be a kaon or a higher resonance, subsequently decaying through strong interaction with a kaon in the final state containing the original $\bar{s}$-quark. So, there is a strong correlation between the charge of the kaon and the 'beauty' [3] of the primary quark. A K^+ is accompanying a $\bar{b}s$ system, whereas a K^- indicates $b\bar{s}$ production. The presence of a strange b-hadron is not the only possibility to create a kaon as particle closest to the b-hadron in the fragmentation chain. The creation of a $u\bar{u}$ ($d\bar{d}$) pair at the first breakup of the string and of a $s\bar{s}$ pair at the following one gives a B^+ (B_d^0) accompanied by a negatively charged (neutral) strange hadron. Thus, the correlation between the charge of the kaon and the beauty of the b quark can be used to discriminate between the cases, whether the primary b-hadron carries strangeness or not (see figure 2a and 2b respectively). To tag the beauty of a b-hadron, information from the same or opposite hemisphere can be used, like jet charge or charge and (transverse) momentum of a high p_t lepton.
For the following discussion, it is useful to introduce a quantity called the 'rank' of a particle. It gives the position of the particle in the fragmentation chain. If the rank zero is assigned to the hadron containing the primary quark in the hemisphere, the following particles are numbered according to their appearance in the fragmentation chain. The rapidity

$$y = \frac{1}{2} \log \frac{E + p_l}{E - p_l}$$

where p_l is the longitudinal momentum of the track with respect to the thrust axis and E its energy, is used as a quantity sensitive to the rank of the particle. Particles with a lower rank are expected to have larger rapidities. In figure 3a, the rapidity distributions of charged tracks are shown for the simulation, separately for B-decay particles, particles with rank 1, called the fragmentation 'sister' of the primary hadron, and remaining fragmentation particles. The three sources of tracks are well separated in this quantity. It should be mentioned that a production rate measurement based on properties of the fragmentation particles is sensitive to the primary rate of strange b-hadrons and not only to the rate of the weakly decaying ones as it is the case for the values deduced, when comparing the two measurements of the mixing parameter χ. This plays an important role and has to be taken into account because the presence of excited B_s^{**} mesons modifies these values. The decay $B_s^{**} \to B_{u,d}^{(*)} K$ dominates because $B_s^{**} \to B_s^{(*)} \pi$ is forbidden by

[3] For commodity of phrasing, a quantity named the 'beauty' has been introduced which is equal to +1 for a b-quark and -1 for a $\bar{b}$-quark.

isospin conservation. Thus, primary produced B_s^{**} mesons migrate to non-strange weakly decaying hadrons giving a non negligible effect if their production rates are large (see also figure 1 and table 1). OPAL and DELPHI have found experimental evidence for these states [12]. Values for $\sigma_{B^{**}_{u,d}}/\sigma_{B_{u,d}}$ around 30% have been measured [12,13] and the results from OPAL and DELPHI are roughly consistent with a similar ratio in the strange sector (details later). The decay $B^{**}_{u,d} \to B_s K$ is not possible because of the masses involved, and can not provide an additional source for strange b-hadrons.
The strategy for the measurement is the following: $b\bar{b}$ events are selected by requiring the output of the confidence method described in chapter 2.1 to be larger than 0.99 when testing the $b\bar{b}$ hypothesis. This gives an efficiency for tagging $b\bar{b}$ events $\epsilon_b \approx 50\%$, with background contaminations of $\epsilon_c \approx 2\%$ and $\epsilon_{uds} < 0.1\%$. A secondary decay vertex is fitted in each hemisphere. The separation between the primary and secondary vertex had to be larger than three standard deviations. Particles tagged as 'standard' kaons are selected. Consistency with the primary event vertex (probability > 0.1) and inconsistency with the secondary decay vertex (probability < 0.1) is required. To tag the beauty of the hemisphere, a neural net is used, which has jet charge and (transverse) momentum of identified leptons as most important input variables. It has been trained to give the output value $1(-1)$ for hemispheres containing a $\bar{b}(b)$ quark. Mixing, especially of B_s mesons with $\chi \approx 0.5$, dilutes the separation power, since the input variables are mainly sensitive to properties of the weakly decaying hadron. To exploit the beauty-charge correlation explained above, the variable $Q_K \times (O_{oppo} - O_{same})$ is used, where $O_{oppo,same}$ is the output of the neural net for the opposite or same hemisphere. The mean value of this quantity is negative (positive) if a charged kaon accompanies a strange (non-strange) meson as it is shown in figure 3b for the simulation. The rapidity is used to be sensitive to the rank of the kaon in the fragmentation chain. To extract the production rate of strange b-hadrons, the two dimensional distribution of the rapidity versus $Q_K \times (O_{oppo} - O_{same})$ is fitted to the shapes for the different contributions obtained from the simulation. These are:

- 'ordinary' fragmentation tracks, not being the 'sister' with rank 1 of the b-hadron,
- the fragmentation 'sister' of the b-hadron, separately for strange and non-strange b-hadrons,
- tracks from B-decays, which pass the cuts for the primary vertex selection, also separately for strange and non-strange b-hadrons,
- background from non $b\bar{b}$ events. This background is very low and its contribution has been fixed in the fit to the value obtained in the simulation.

The binned fit is based on a log-likelihood method taking into account the limited statistics of the simulation sample [14]. The result of the fit is shown in figure 4 for the projections onto the rapidity (4a) and $Q_K \times (O_{oppo} - O_{same})$ (4b). The cuts for the selection of tracks from the primary vertex and for the kaon identification (using the 'loose' and 'tight' tag) have been varied, and the quantity $Q_K \times (O_{oppo} - O_{same})$ has been replaced by $Q_K \times (Q_{Jet,oppo} - Q_{Jet,same})$, using only jet charge information. The statistical error of the ratio r (see chapter 4) has been taken as systematic error. The result for the rate of primary produced strange mesons, denoted f'_{B_s} in the following is:

$$f'_{B_s} = (12.0 \pm 1.4(\text{stat.}) \pm 2.5(\text{syst.}))\%$$

Further studies of systematic errors are in progress.

This measurement allows a determination of the parameter γ_s in the JETSET model which gives the suppression of $s\bar{s}$ pairs in the fragmentation with respect to $u\bar{u}$, $d\bar{d}$ pairs: $\gamma_s = P(s\bar{s})/P(u\bar{u}) = P(s\bar{s})/P(d\bar{d}) = f'_{B_s}/f'_{B_u} = f'_{B_s}/f'_{B_d}$. From

$$f'_{B_s} = \frac{\gamma_s \cdot (1 - f'_{b-Baryon})}{2 + \gamma_s} \tag{1}$$

one gets

$$\gamma_s = 0.31 \pm 0.09(f'_{B_s}) \pm 0.01(f'_{b-Baryon}). \tag{2}$$

It should be mentioned, that this method is measuring γ_s at a given position in the fragmentation process, namely at the beginning of the fragmentation chain, where the quark from the Z^0 decay is involved.

To deduce a value for the rate f_{B_s} of weakly decaying B_s-mesons, assumptions for the rate of B_s^{**}-mesons have to be made. The signals giving experimental evidence for these states have large uncertainties [12][4]:

$$\frac{BR(\bar{b} \to B_s^{**})}{BR(\bar{b} \to B_s)} = 0.175 \pm 0.052 \quad (\text{OPAL}), \tag{3}$$

$$\frac{BR(\bar{b} \to B_{s1}, B_{s2}^*)}{BR(\bar{b} \to B_s)} = 0.33 \pm 0.14 \quad (\text{DELPHI}). \tag{4}$$

$B_{u,d}^{**}$ mesons have been reconstructed with much larger statistics [12,13]. The composition of the signals is not known. So, it is not clear, whether only narrow states or also broad states contribute and their relative production rates are not precisely known. Furthermore, possible decays $B^{**} \to B^{(*)}\rho$ give an additional source of these mesons. In inclusive analyses, the relative B^{**} rates have been measured to be[5]:

$$\sigma_{B_{u,d}^{**}}/\sigma_{B_{u,d}} = 0.27 \pm 0.06 \quad (\text{OPAL}), \tag{5}$$

$$= 0.35 \pm 0.08 \quad (\text{DELPHI}), \tag{6}$$

$$= 0.28 \pm 0.08 \quad (\text{ALEPH}). \tag{7}$$

For these results, different assumptions for the composition of the signals have been made. ALEPH computed their central value using the hypothesis that only narrow states with a relative faction of 67% contribute to the observed signal. If also broad states contribute with the same efficiency, the value goes down to 19%.
For the determination of f_{B_s}, the following value for the B_s^{**} rate is used, covering the range of the experimental results given above:

$$P_{B_s^{**}} = \frac{BR(b \to B_s^{**})}{BR(b \to B_s^{**} + B_s^{(*)})} = 0.27 \pm 0.08. \tag{8}$$

Using this number, one gets

$$f_{B_s} = (8.8 \pm 1.0(\text{stat.}) \pm 1.8(\text{syst.}) \pm 1.0(B_s^{**}\text{ rate}))\%. \tag{9}$$

[4]The DELPHI result has been computed using the given number for $(\sigma_{B_{s1}} + \sigma_{B_{s2}^*})/\sigma_{B_{u,d}^{**}} = 0.142 \pm 0.055$ and the measured $B_{u,d}^{**}$ rate. A value of 11.2% has been assumed for the total production rate of strange B mesons. B_{s1} and B_{s2}^* are the B_s^{**} states with quantum numbers $J^P = 1^+$ and $J^P = 2^+$ ($j_q = l_q + s_q = 3/2$ for both) which are expected to be narrow.

[5]In the OPAL analysis, only final states with a charged B-meson have been taken into account. This has been corrected using the isospin amplitudes of the strong decays.

4 Test of fragmentation properties in charm events

The method used for the measurement of the fraction of strange b-hadrons relies heavily on the fragmentation model, since rapidity distributions and charge correlations have been used for this measurement. The JETSET model with string fragmentation has been used to extract the distributions for the different sources which have been fitted to the data. This model has been well tuned to describe quantities being sensitive to fragmentation effects [7]. Analyses studying particle-particle correlations and the structure of the fragmentation chain also exist [15, 16]. The goal of the analysis described in this chapter is to study properties of fragmentation particles in $c\bar{c}$ events and to compare them with the Monte Carlo model. $c\bar{c}$ events have been chosen for these studies, because they offer two main advantages:

- The situation is expected to be similar for $b\bar{b}$ events, because the primary produced $q\bar{q}$ pair is heavy ($m_Q >> \Lambda_{QCD}$) and thus also has a hard fragmentation function. If the simulation describes the data well in $c\bar{c}$ events, this should also be the case in $b\bar{b}$ events,

- The primary hadron and the particles stemming from fragmentation can be tagged with low background by reconstructing exclusive decays of D mesons.

The decay $D^{*+} \to D^0\pi^+ \to K^-\pi^+\pi^+$ has been reconstructed by fitting a common vertex with all combinations of three tracks with the correct charge and having at least one vertex detector hit. The mass of the $K^-\pi^+$ system for the D^0 candidate had to be within 50 MeV around the nominal D^0 mass of $m_{D^0} = 1864.5$MeV [1]. To reduce the background of D^{*+} mesons from $b\bar{b}$ events, the following cuts have been applied (figure 5):

- The momentum fraction $x_p = p_{D^*}/p_{beam}$ had to be larger than 0.4. D-mesons have large momenta because of the hard c-fragmentation function whereas D-mesons from B-decays have a softer momentum spectrum.

- The probability for all tracks in the hemisphere, excluding the D^* decay tracks, to originate from the primary vertex had to be larger than 5%. In case of b-hadrons, because of their larger decay multiplicity, it is expected to find additional tracks in the hemisphere coming from the secondary decay vertex, thus giving a lower probability value.

- The tracks in the opposite hemisphere are sorted by increasing order $1, 2, \ldots, n$ of consistency with the primary vertex. The mass $m_{1,i}$ is calculated for the system formed with tracks $1, 2, \ldots, i$. The primary vertex probability for track $i+1$ which gives $m_{1,i+1} > 1.8$ GeV had to exceed 5%.

With these cuts, an efficiency for selecting $c\bar{c}$ events of $\approx 60\%$ with a rejection factor against $b\bar{b}$ events of ≈ 11 is achieved using simulated events. The resulting mass difference spectrum ($\Delta m = m_{K\pi\pi} - m_{K\pi}$) is shown in figure 6 together with the small remaining contamination from $b\bar{b}$ events, estimated from the simulation. 1123 ± 37(stat.) reconstructed D^* decays can be found in this sample. D^* candidates with $|\Delta m - 145.5 \text{ MeV}| < 1$ MeV have been selected. The overall rapidity distributions of D^* decay products and fragmentation particles are shown in figure 7. They agree well in data and simulation. To test

the correlation between the charge of a fragmentation particle and the 'charm' [6] of the D-hadron, several quantities have been studied separately for tracks with charge of opposite and same sign as the D^* meson. Pions from the decay of orbitally excited D-mesons, especially $D_1(2420) \to D^{*+}\pi^-$, have opposite charge than the D^* and preferably large rapidity. Thus, their presence will affect the distributions studied in the following. To reject them, tracks were not accepted if their masses with the D^* was around the mass of the $D_1(2420)$. Figure 8 shows the rapidity difference $\Delta y = y_{D^*} - y_i$ (8a) and the rank[7] for the two samples (8b). Particles with opposite charge are found more often close to the D^*. This is visible at low values for the rank and the rapidity difference where a significant excess of oppositely charged particles is found. Thus, the expected behaviour can be clearly observed in data and is well described by the simulation. A further test can be done by looking e.g. at the rapidity gap between two particles produced in the fragmentation. Figure 8c shows the rapidity gap $y_i - y_{i+1}$ where i denotes the rank of a particle. The agreement between data and simulation is also satisfactory.
To look for the kaon which is expected to compensate the strangeness of a strange primary hadron, D_s mesons have been reconstructed in the channels $D_s^+ \to \Phi\pi^+ \to K^+K^-\pi^+$ and $D_s^+ \to \bar{K}^*K^+ \to K^-\pi^+K^+$. To enrich the selected sample in $c\bar{c}$ events the same cuts as described above have been applied. The mass spectrum for this sample is shown in figure 9a. It contains 207 ± 20(stat.) reconstructed D_s decays. Kaons have been selected by requiring the 'standard' tag from the combined TPC and RICH information. The sidebands have been used to subtract the combinatorial background under the signal, not stemming from D_s decays. One gets an excess of oppositely charged kaons at low values of the rank as expected (figure 9b). Subtracting the same-sign from the opposite-sign distribution in data and simulation, summing up the first 3 or 4 bins, where the fragmentation 'sister' is expected, as it can be seen in figure 8b and defining:

$$r = \frac{\sum_{i=1}^{3,4}(\#\text{oppos. sign} - \#\text{same sign})_{sim.}}{\sum_{i=1}^{3,4}(\#\text{oppos. sign} - \#\text{same sign})_{data}}$$

allows a more quantitative evaluation, whether the simulation describes the presence of the accompanying kaon properly. The result is $r = 1.2 \pm 0.2$(stat.), showing a possible higher excess of opposite sign kaons in simulation than in data, nevertheless being consistent with unity.

5 Measurement of the rates of neutral and charged b-hadrons

For this analysis, about 1.4 Million multihadronic events from the 1994 run were used. Events with 2 jets covered by the vertex detector ($|\cos\theta_{thrust}| < 0.7$) were selected. The tagging of $b\bar{b}$ events was performed in the hemisphere opposite to the one which was used for the measurement. The output of the confidence method had to be larger than 0.99, giving a b-purity of about 98.4%. A secondary vertex was fitted in the hemisphere. Hadronic interactions in the detector material were reconstructed using the algorithm

[6] The 'charm' is defined in the same way for c-quarks as the 'beauty' for b-quarks.

[7] The rank used here is different from the one defined in chapter 3. Here, the rank denotes the numbering of the tracks in a hemisphere, if they are sorted by decreasing order of rapidity.

described in [17]. Since the track causing the interaction is lost in most of the cases, hemispheres with such interactions were rejected.
The basic idea to measure the rates of charged and neutral b-hadrons is to reconstruct the charge of the weakly decaying hadron. Based on a neural network, for each track in a hemisphere a probability P_B is calculated that it originates from a b-hadron decay rather than from fragmentation. Input variables are the probability that the track fits to the primary vertex, the momentum, the rapidity of the track with respect to the thrust axis, the reconstructed flight distance in the $R\phi$ plane and its error. The latter two are not specific for the tracks but for the hemisphere considered. They give additional information about the separation power of the other variables, especially the vertex probability. The distributions of the netoutput variable are shown in figure 10. Tracks are accepted if their momentum exceeds 500 MeV and at least one vertex detector hit has been associated. At least four tracks had to be accepted in the hemisphere. The maximum number of tracks in the hemisphere failing these acceptance cuts was limited (compare table 2). A secondary vertex charge is then constructed through:

$$Q_B = \sum_{i=1}^{N_{hem}} Q_i P_{B,i}. \tag{10}$$

Assuming binomial statistics, an error on Q_B can be defined as

$$\sigma_{Q_B} = \sqrt{\sum P_B(1 - P_B)} \tag{11}$$

This quantity does not account for track losses due to inefficiencies in the track reconstruction. σ_{Q_B} is small if all tracks are well classified, having values of P_B close to 0 or 1, and gets larger the more tracks have probabilities around 0.5. Parameters in the simulation possibly having an effect on the measurement had to be adjusted. These are:

- Lifetimes of b-hadrons. The averages from [18] have been used.
- The rates of different b-hadron species from [2] because different b-hadrons contribute to a certain charge (e.g. B_d, B_s, Λ_b, Ξ_b^0 to $Q = 0$). Their distributions look slightly different.
- The integrated mixing probability χ_d for B_d-mesons from [2] to take into account the effect of different Q_B shapes for B_d and $\bar{B}_d$.
- The rates of excited b-hadrons, namely orbitally excited $B^{**}_{u,d,s}$-mesons and $\Sigma_b^{(*)}$-baryons. The expected strong decays of these states produce particles (pions or kaons) looking partly fragmentation like (stemming from the primary vertex) and partly B-decay like (large rapidity). For $P_{B^{**}_{u,d,s}}$ the estimate from equation 8 is used. Since there exists only one measurement with large uncertainties for $\Sigma_b^{(*)}$ production [19] which has not yet been confirmed, the following value is taken as a conservative choice [8]: $P_{\Sigma_b^{(*)}} = 0.30 \pm 0.15$.

The values of these parameters are also summarised in table 2. The shapes of the Q_B distributions are directly affected by the number of tracks which have been used in the

[8] $P_{\Sigma_b^{(*)}}$ is defined in the same way as $P_{B^{**}}$.

reconstruction of the vertex charge. This number is larger in data than in simulation by 0.16 at a mean value of about 7.6. The simulated events are reweighted to get agreement in this distribution. The error of the vertex charge, defined in equation 11, also influences the Q_B distributions. The mean value of the σ_{Q_B} in dependence of the number of tracks is shown in figure 11. Data and simulation agree well, the deviations are below 3%. The simulated events are reweighted to get the σ_{Q_B} distributions in agreement, individually for any number of tracks. To control the loss of charged tracks, the number of tracks in the hemisphere not passing the track cuts are also brought into agreement. It has to be mentioned that all these corrections are small. Comparing the Q_B distributions of data and simulation shows a slight shift towards positive values of the data distribution with respect to the simulation by 0.0063 which is corrected.
The measured Q_B distribution has been fitted to the corresponding shapes expected for charged an neutral b-hadrons obtained from the simulation. The technique already mentioned in chapter 3 and described in [14] has been used. The non $b\bar{b}$ background has been fixed to the value obtained from simulation. The real data distribution together with the fit result and the simulation prediction for neutral, positively and negatively charged b-hadrons is shown in figure 12. The result for $f^+ = BR(\bar{b} \to X_B^+)$ is:

$$f^+ = (42.48 \pm 1.06(\text{stat.}))\%.$$

$f^0 = BR(\bar{b} \to X_B^0)$ is given through $f^0 = 1 - f^+$. To estimate systematic errors, parameters in the simulation and cuts have been varied, the input to the neural network has been changed (e.g. using only vertexing variables). The breakdown of the systematic errors is shown in table 2. Systematic effects due to uncertainties in the modelling of b-hadron decays remain to be studied. The preliminary result including systematic errors is:

$$f^+ = (42.48 \pm 1.06(\text{stat.}) \ \pm 1.03(\text{syst.}))\%.$$

As a cross-check the distribution of negatively and positively charged b-hadrons have been fitted separately. This gives

$$\begin{aligned} BR(b,\bar{b} \to X_B^+) &= (21.23 \pm 0.63(\text{stat.}))\% \\ BR(b,\bar{b} \to X_B^-) &= (21.25 \pm 0.62(\text{stat.}))\%. \end{aligned}$$

The two numbers are correlated ($\rho^{\pm} = 0.49$). The vertex charge in dependence of the direction of the thrust axis is shown in figure 13, reflecting the $b\bar{b}$ forward-backward asymmetry.

6 Interpretation of results

Combining the value for f_{B_s} found in this analysis with the number given in [2] gives (assuming uncorrelated errors and adding the different sources in quadrature):

$$f_{B_s} = (10.3 \pm 1.2)\%. \tag{12}$$

Weakly decaying neutral b-hadrons are B_d^0 and B_s mesons, the Λ_b baryon and some fraction of strange b baryons (Ξ_b^0). The rate of charged b-hadrons is dominated by the B^+ meson, strange baryons only give a minor contribution (Ξ_b^-, Ω_b). Formally, one gets:

$$\begin{aligned} f^0 &= f_{B_d^0} + f_{B_s} + f^0_{b-Baryon}, \\ f^+ &= f_{B_u^+} + f^+_{b-Baryon}. \end{aligned} \tag{13}$$

source	value and variation	$\delta f^+[\%]$
τ_{B^+}	1.66 ± 0.03 ps	0.17
τ_{B^0}	1.55 ± 0.03 ps	0.07
τ_{B_s}	1.47 ± 0.06 ps	0.04
$\tau_{b-baryon}$	1.19 ± 0.05 ps	0.02
χ_d	0.175 ± 0.009	0.08
$P_{B^{**}}$	0.27 ± 0.08	0.36
$P_{\Sigma_B^{(*)}}$	0.30 ± 0.15	0.15
f_{B_s}	10.8 ± 1.4 %	0.31
$f_{b-Baryon}$	10.2 ± 2.3 %	0.08
$f_{B_d^0} = f_{B_u^+}$	39.5 ± 1.4 %	0.11
non bb background	1.55 ± 0.78 %	0.26
BCONF opp. hemisphere	0.99-0.999	0.23
$\lvert\cos\theta_{thrust}\rvert$	0.6-0.7	0.08
min. # of acc. tracks	3-5	0.12
max. # of rej. tracks	3-5	0.50
variation of fitrange	$\lvert Q_B\rvert < 2-4$	0.03
selection of NN input variables		0.60
sum		1.03

Table 2: Breakdown of systematic errors on f^+.

With some assumptions about the rate of charged b-baryons, $f_{B_u^+}$ can be extracted from f^+ with small additional uncertainties. These relative fractions of charged and neutral b baryons are taken from simulation (compare table 1):

$$f^0_{b-Baryon} = 0.93 \cdot f_{b-Baryon}, \quad f^+_{b-Baryon} = 0.07 \cdot f_{b-Baryon}. \tag{14}$$

With the errors on $f_{b-Baryon}$ from [2] and assigning a 50% relative error on $f^+_{b-Baryon}$, one gets:

$$f_{B_u^+} = (41.77 \pm 1.48(f^+) \pm 0.39(f_{b-Baryon}, f^+_{b-Baryon}))\%.$$

To get the best estimate of all b-hadron rates, available measurements for f_{B_s}, $f_{b-Baryon}$, f^0 and f^+ have to be put together using the conditions $f_{B_s} + f_{b-Baryon} + f_{B_d^0} + f_{B_u^+} = 1$ and $f_{B_d^0} = f_{B_u^+}$. The latter one can also be dropped, because there are enough measurements to determine $f_{B_d^0}$ and $f_{B_u^+}$ separately. Possible sources of different rates for B_d^0 and B^+ mesons could be:

- Different rates of the ground state mesons B_d^0 and B^+ produced in the fragmentation.
- Influence of strongly decaying excited b hadrons, especially B^{**} mesons. This could be caused by electroweak contributions to the decay amplitude modifying the strong isospin amplitudes or phase space effects due to the masses involved (e.g. $m_{K^\pm} - m_{K^0} \approx 4$ MeV might slightly enhance the production of charged B-mesons over neutral ones in B_s^{**} decays).

7 Conclusions

Measurements of the rates of strange, neutral and charged b-hadrons have been presented in this paper. For the determination of the strange b-hadron rate, a method has been used which is complementary to existing measurements. It exploits properties of the fragmentation kaon accompanying the strange b-hadron. Thus, this method is sensitive to the primary strange b-hadron rate, f'_{B_s}, whereas analyses based on the mixing parameter χ or inclusive branching ratios measure the rate of weakly decaying B_s-mesons, f_{B_s}. The result is $f'_{B_s} = (12.0 \pm 1.4(\text{stat.}) \pm 2.5(\text{syst.}))\%$. A relative B_s^{**} rate of $(27 \pm 8)\%$ leads to $f_{B_s} = (8.8 \pm 1.0(\text{stat.}) \pm 1.8(\text{syst.}) \pm 1.0(B_s^{**} \text{ rate}))\%$, in good agreement with the number given in [2]. The rates of charged weakly decaying b-hadrons have been measured to be $f^+ = (42.48 \pm 1.06(\text{stat.}) \pm 1.03(\text{stat.}))\%$. With assumptions for the rate of charged b-baryons, $f_{B_u^+}$ has been extracted to be $f_{B_u^+} = (41.77 \pm 1.48(f^+) \pm 0.39(f_{b-Baryon}, f^+_{b-Baryon}))\% = (41.77 \pm 1.53)\%$, if errors are added quadratically. This measurement adds substantial input for a combination of measurements to estimate b-hadron rates. Furthermore, tests of the fragmentation process have been performed using exclusively reconstructed D-mesons in a sample enriched in $c\bar{c}$ events. All results are preliminary.

References

[1] Particle Data Group, Eur. Phys. J. **C 3**, (1998), 1.

[2] The LEP B Oscillations Working group, LEPBOSC NOTE 98/3.

[3] DELPHI Collaboration, Phys. Lett. **B289** (1992) 199,
OPAL Collaboration, Phys. Lett. **B295** (1992) 357,
ALEPH Collaboration, Phys. Lett. **B361** (1995) 221.

[4] DELPHI Collaboration, Zeit. Phys. **C68** (1995) 375,
DELPHI Collaboration, Zeit. Phys. **C68** (1995) 541,
ALEPH Collaboration, Phys. Lett. **B384** (1996) 449,
ALEPH Collaboration, Eur. Phys. J. **C 2** (1998) 197.

[5] ALEPH Collaboration, Eur. Phys. J. **C 5** (1998) 205.

[6] T. Sjöstrand, Computer Physics Communications **82** (1994) 74.

[7] DELPHI Collaboration, Zeit. Phys. **C73** (1996) 11.

[8] DELSIM User's Guide, DELPHI Note 89-15 PROG 130,
DELSIM Reference Manual, DELPHI Note 89-68 PROG 143.

[9] DELPHI Collaboration, Nucl. Instr. and Meth. **A303** (1991) 233.

[10] DELPHI Collaboration, Nucl. Instr. and Meth. **A378** (1996) 57.

[11] W.J. Murray, "Improved B tagging using Impact Parameters", DELPHI Note 95-167 PHYS 581.

[12] OPAL Collaboration, Z. Phys. **C66** (1995) 27,
DELPHI Collaboration, contr. EPS0563, EPS Conference Brussels 1995.

[13] DELPHI Collaboration, Phys. Lett. **B345** (1995) 598,
ALEPH Collaboration, Z. Phys. **C69** (1996) 393,
ALEPH Collaboration, contr. PA01-070, ICHEP'96 Warsaw 1996.

[14] R. Barlow, C. Beeston, Computer Physics Communications **77** (1993) 219.

[15] OPAL Collaboration, Phys. Lett **B305** (1993) 415;
DELPHI Collaboration, Phys. Lett **B318** (1993) 249;
ALEPH Collaboration, Zeit. Phys. **C64** (1994) 361;
DELPHI Collaboration, Phys. Lett **B416** (1998) 247.

[16] DELPHI Collaboration, Phys. Lett. **B407** (1997) 174.

[17] C. Weiser, PhD thesis, IEKP-KA/98-5, University of Karlsruhe;
MAMMOTH, http://home.cern.ch/ pubxx/tasks/elephant/www/mammoth/Welcome.html

[18] The b-hadron lifetime group, Averages of b-hadron lifetimes for winter 99 conferences

[19] DELPHI Collaboration, contr. EPS0565, EPS Conference Brussels 1995.

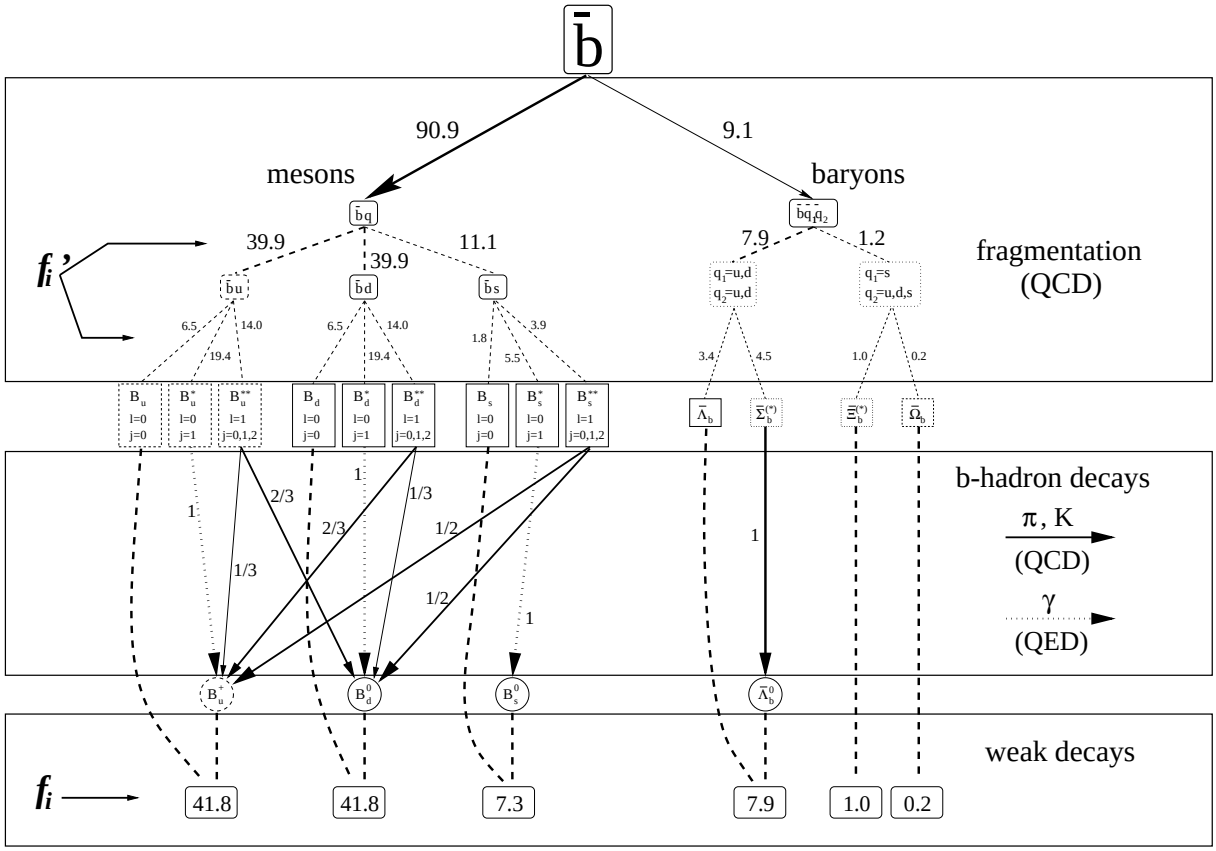

Figure 1: Schematic picture of the production mechanism of b-hadrons. The rates of hadrons primarily produced in the fragmentation are denoted f', the ones which are decaying through weak interaction f. Strong and electromagnetic decays are indicated by solid and dotted arrows, respectively, together with their (expected) branching ratios (For strong decays only single pion and kaon transitions have been taken into account). The given rates are taken from simulation (compare with table 1).

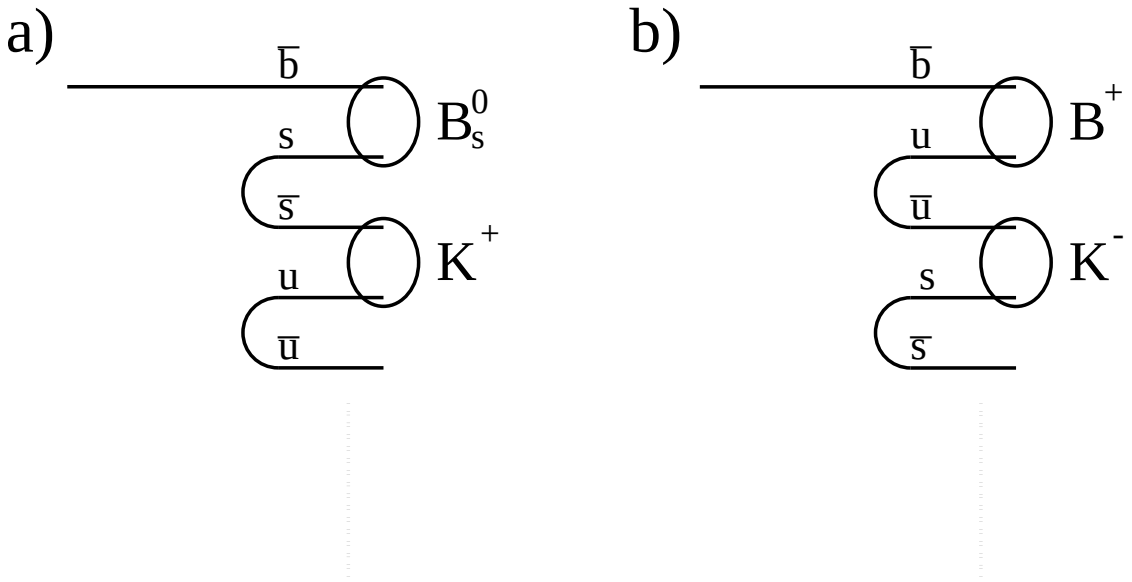

Figure 2: The creation of a kaon as 'sister' particle of the primary b-hadron in the jet fragmentation. In a) the kaon compensates the strangeness of the B_s meson, in b) the B-meson doesn't carry strangeness, and the $\bar{s}$ quark is contained in the particle created later in fragmentation. The two cases can be separated by tagging the beauty of the hemisphere and/or of the opposite hemisphere.

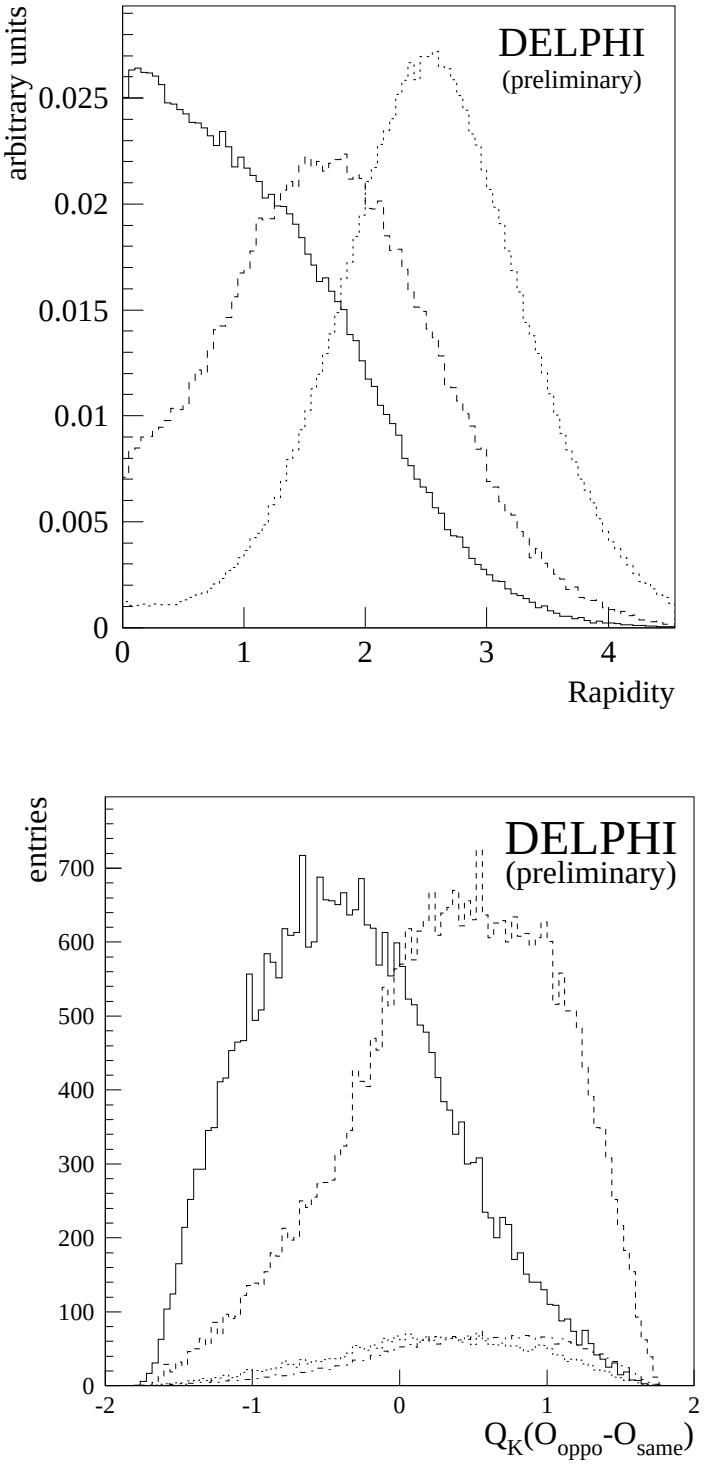

Figure 3: The most important variables for the measurement of the strange b-hadron rate obtained from simulation:
upper: The normalised rapidity distributions for B-decay particles (dotted), the fragmentation 'sister' of the b-hadron (dashed) and other fragmentation tracks (solid histogram).
lower: The quantity $Q_K \times (O_{oppo} - O_{same})$ for kaons accompanying a strange (solid histogram) or non-strange b-hadron (dashed histogram). For the latter case, there is a small difference whether the b-hadron is neutral (dotted) or charged (dash-dotted), where the histograms have been scaled down in size to avoid confusing overlap with the other ones.

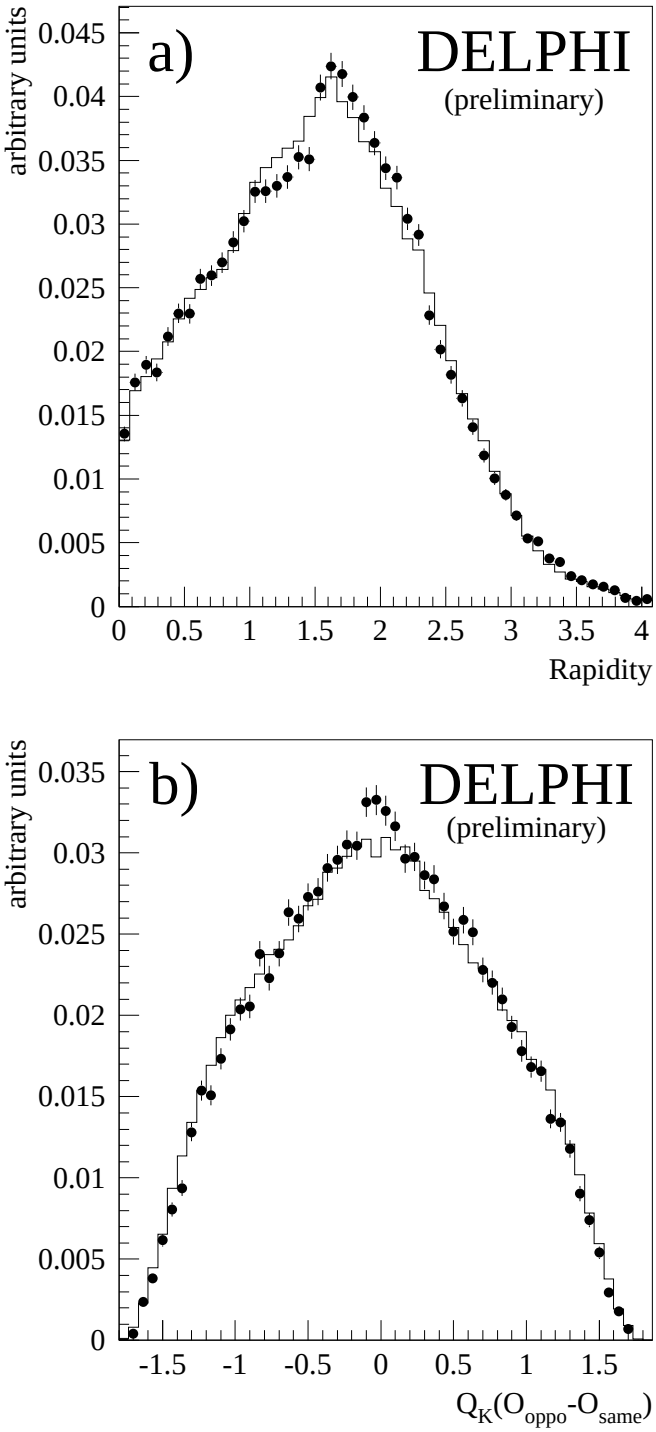

Figure 4: The fit result for the determination of the strange b-hadron rate using identified kaons from the primary vertex as explained in the text. Shown are the data (circles with error bars) with the result of the fit (histogram) superimposed for the projections onto the rapidity (a) and $Q_K \times (O_{oppo} - O_{same})$ (b)

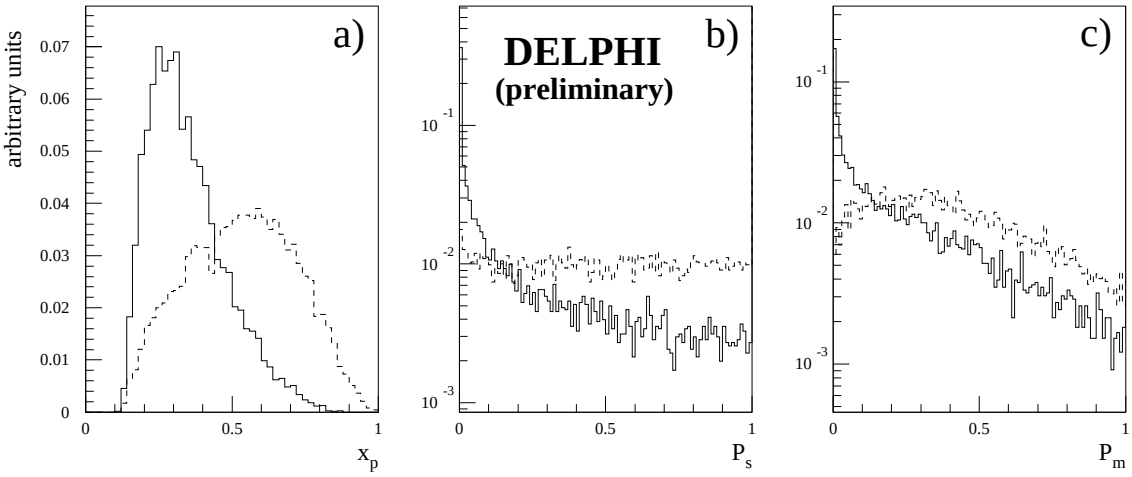

Figure 5: The variables used to reduce the background of D* mesons from $b\bar{b}$ events as described in the text (solid: $b\bar{b}$ events; dashed: $c\bar{c}$ events):
a) $x_p = p_{D^*}/p_{beam}$;
b) probability for tracks in the hemisphere, excluding the D* decay products, to originate from the primary vertex;
c) primary vertex probability in opposite hemisphere for track $i+1$ with $m_{1,i+1} > 1.8$ GeV.

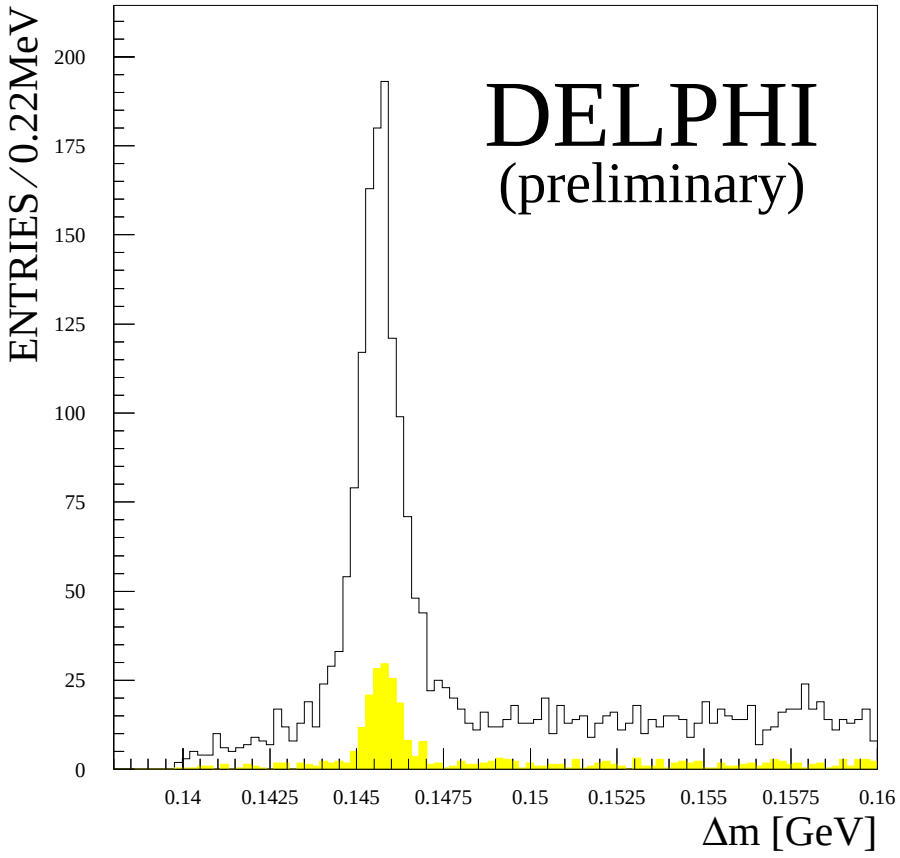

Figure 6: The mass difference spectrum for the D* candidates (data) after applying the cuts for $c\bar{c}$ selection described in the text. The background from $b\bar{b}$ events (shaded area) estimated from the simulation is also shown.

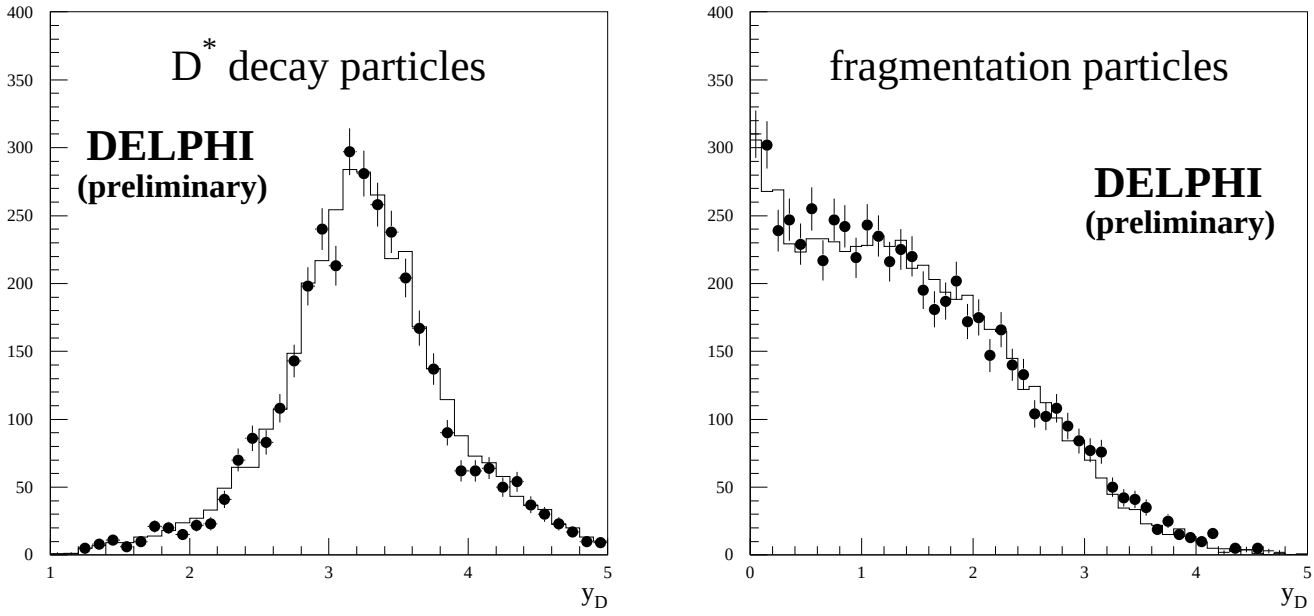

Figure 7: The rapidity distributions for particles stemming from the decay of the D^* meson (left) and for fragmentation particles (right). The data are shown as closed circles with error bars and the simulation as solid histogram. The rapidity has been calculated with respect to the direction of the D^*-meson.

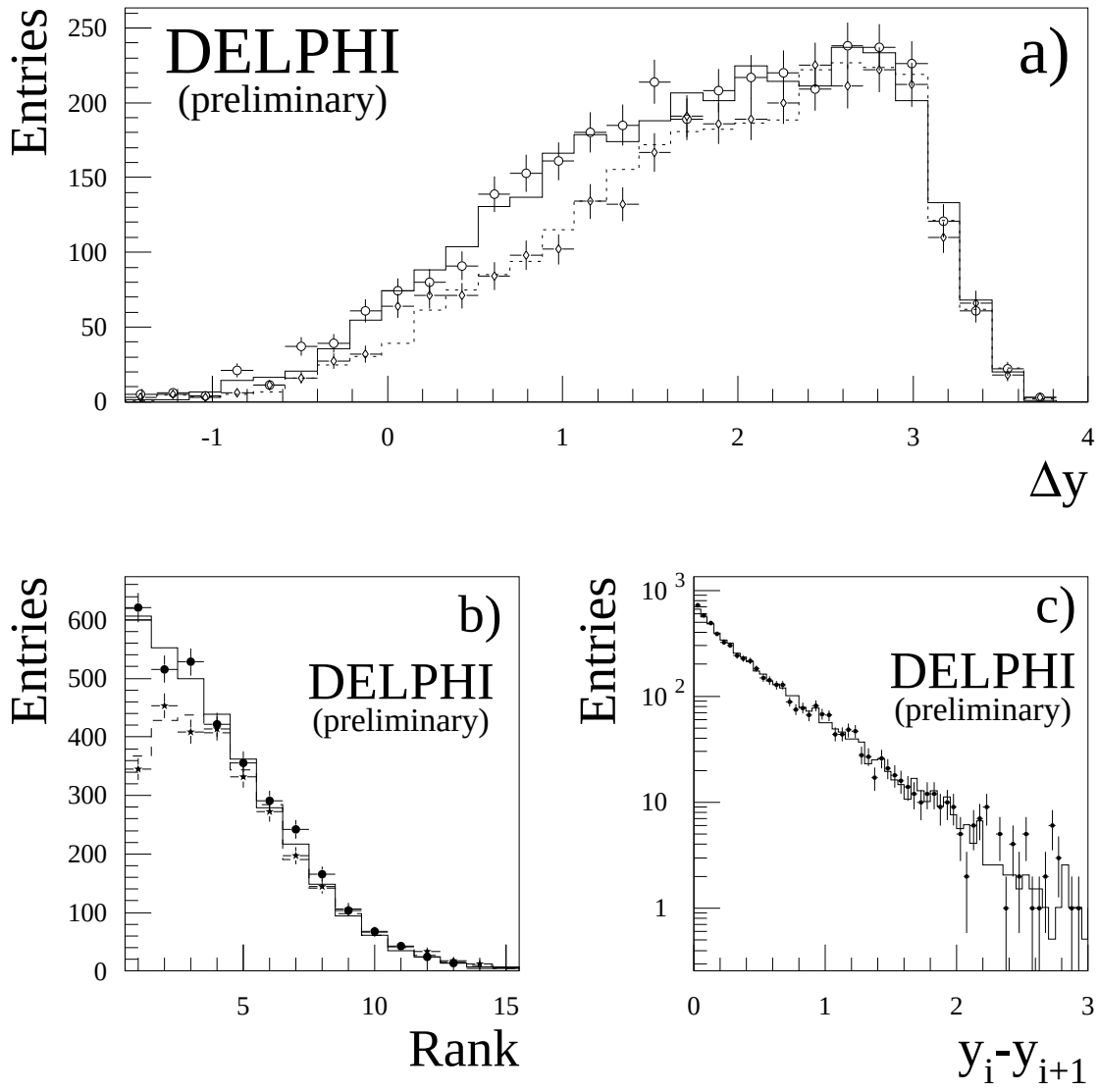

Figure 8: a) The rapidity difference $\Delta y = y_{D^*} - y_i$ for fragmentation tracks with opposite (data: open circles, simulation: solid histogram) and same charge (data: open diamonds, simulation: dashed histogram) as the D^*.
b) The rank as defined in the text for opposite (data: circles, simulation: solid histogram) and same sign (data: stars, simulation: dashed histogram).
c) The rapidity gap between two fragmentation tracks with rank i and $i+1$ for data (circles) and simulation (histogram).

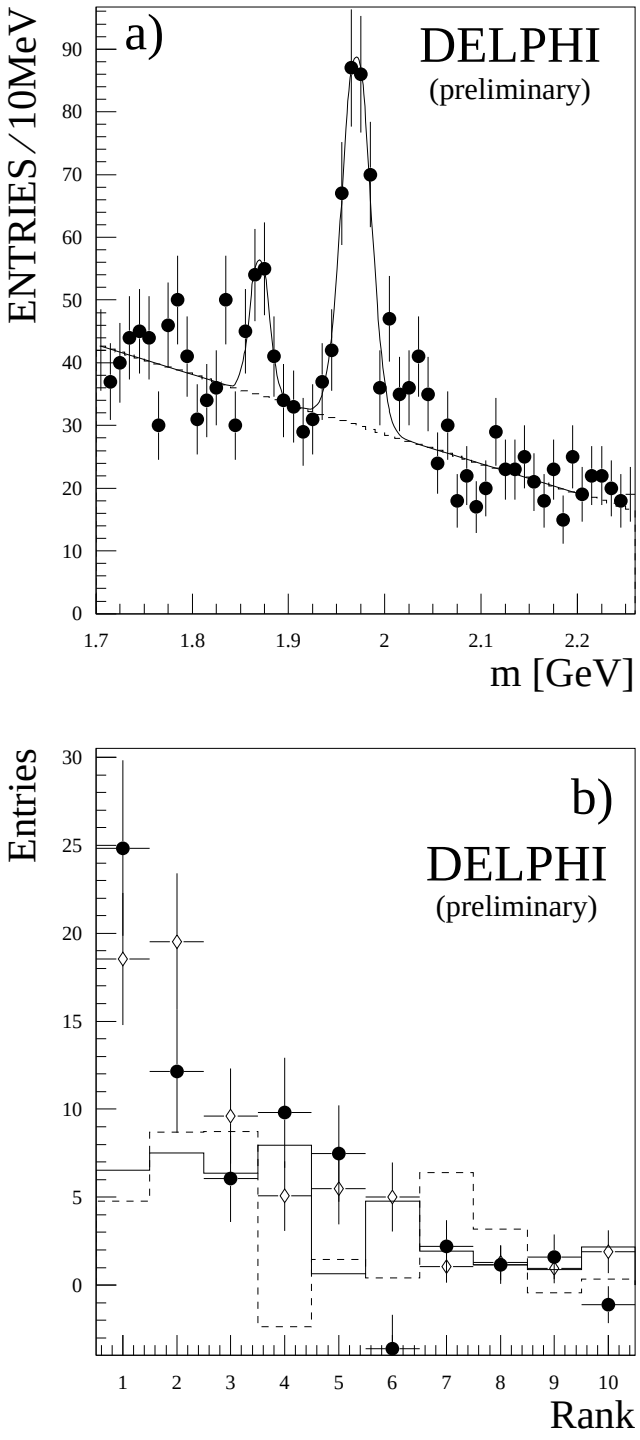

Figure 9: a) The D_s mass spectrum for the $c\bar{c}$-enriched sample (data).
b) The rank for identified kaons with opposite (circles) and same (solid histogram) charge as the D_s-candidate in data and simulation (open diamonds and dashed histogram, respectively).

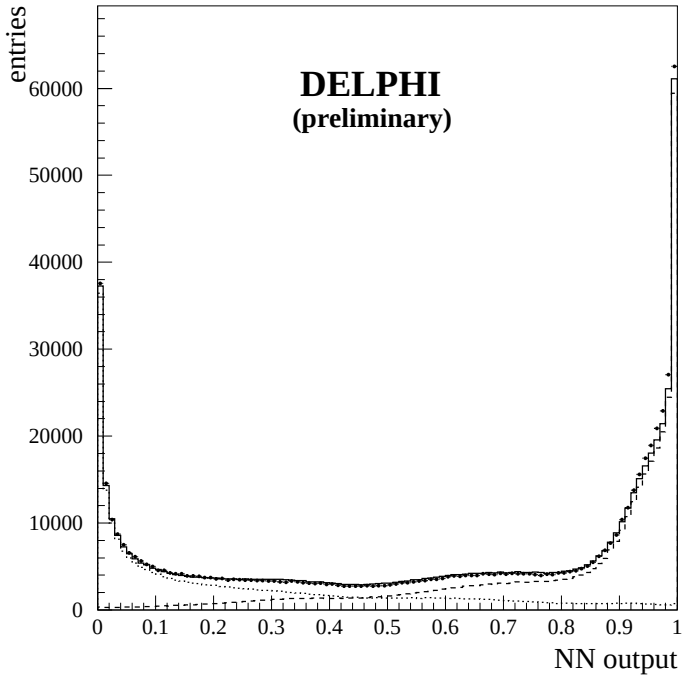

Figure 10: The output of the neural network to separate B decay particles from fragmentation tracks. Shown are the data (closed circles), the simulation (solid histogram) and the contributions from B decay tracks (dashed) and their fragmentation counterparts(dotted).

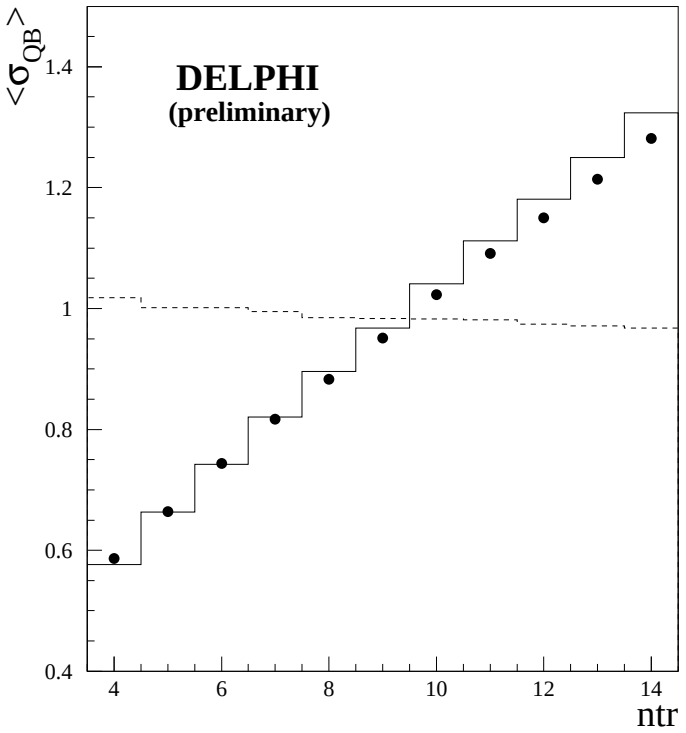

Figure 11: $\langle \sigma_{Q_B} \rangle$ versus number of tracks which have been used for the estimation of the vertex charge for data (closed circles) and simulation (histogram). The ratio $\langle \sigma_{Q_B} \rangle_{data} / \langle \sigma_{Q_B} \rangle_{sim.}$ is shown as dashed line. The deviation is lower than 3% over the whole range.

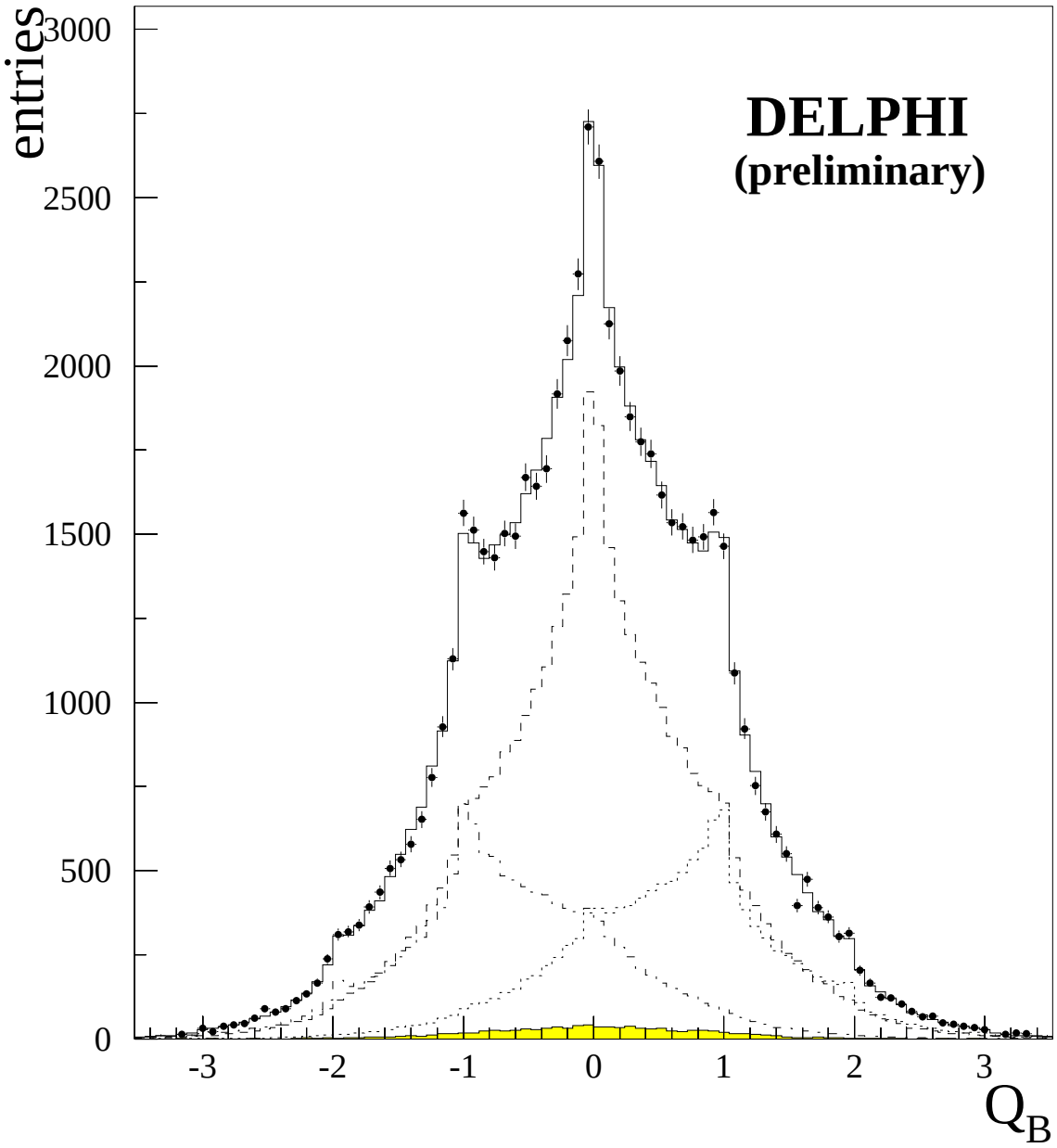

Figure 12: The vertex charge Q_B for the data (points with error bars) with the result of the fit superimposed (solid histogram). The shapes for neutral (dashed histogram), negatively (dashed-dotted) and positively (dotted) charged b-hadrons obtained from the simulation and used in the fit are also shown. The contribution of non $b\bar{b}$ events is given as shaded histogram.

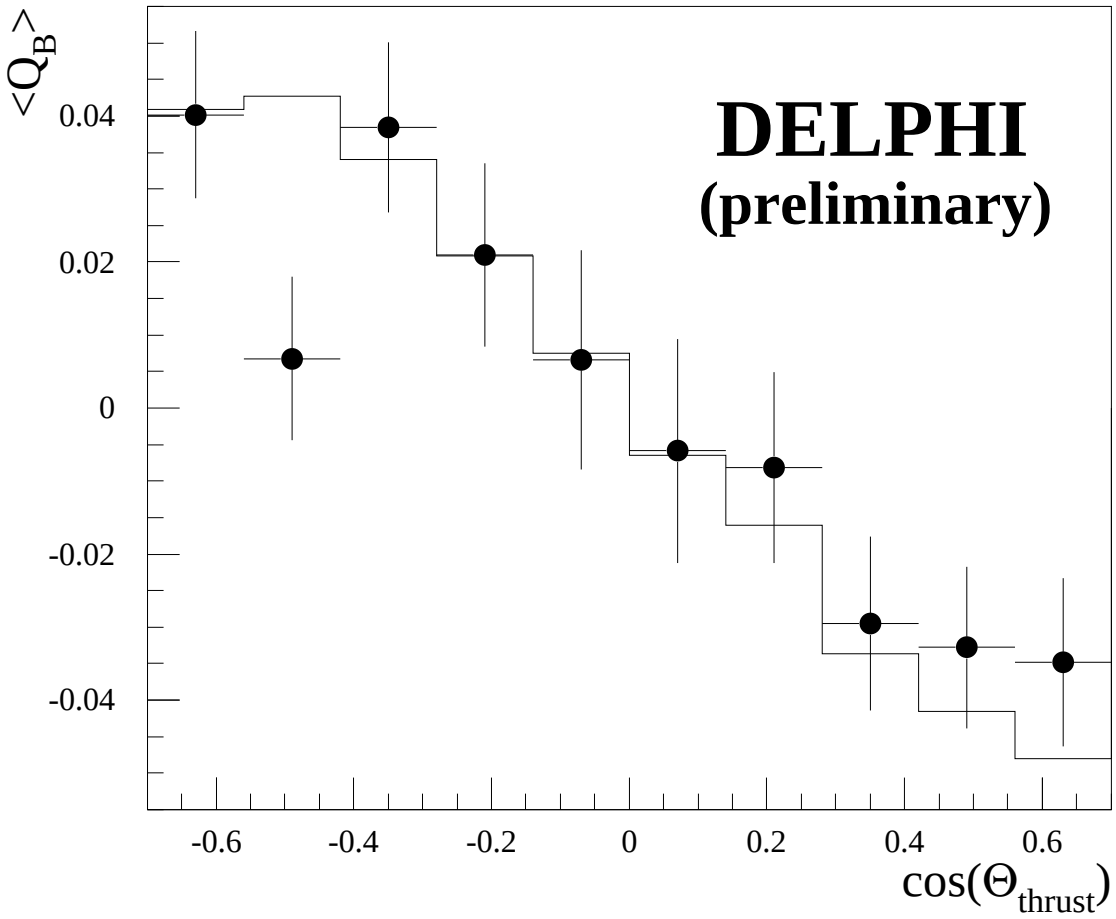

Figure 13: The mean value of the vertex charge in dependence of $\cos\theta_{thrust}$ where the orientation of the thrust axis is given by the hemisphere considered. Shown are the data (closed circles with error bars; the error bars correspond to the root mean square of the Q_B distribution) and simulation (histogram).